0888-8809/06/$15.00/0
Printed in U.S.A.

Molecular Endocrinology 20(4):724–734

doi: 10.1210/me.2005-0419

Glutamic Acid 709 Substitutions Highlight the Importance of the Interaction between Androgen Receptor Helices H3 and H12 for Androgen and Antiandrogen Actions

Virginie Georget, William Bourguet, Serge Lumbroso, Salouah Makni, Charles Sultan, and Jean-Claude Nicolas

Institut National de la Santé et de la Recherche Médicale (INSERM), Unité 540 (V.G., S.L., C.S., J.-C.N.); Centre de Biochimie Structurale (W.B.), Centre National de la Recherche Scientifique (CNRS); Université Montpellier 1, F-34090, Montpellier, France; Laboratoire d'Hormonologie du Développement et de la Reproduction (S.L., C.S.), Hôpital Lapeyronie, Centre hospitalier Universitaire, F34 295, Montpellier, France; and Service de Pédiatrie (S.M.), Hôpital d'Enfants de Tunis, 1000 Tunis, Tunisia

The mutation of a single amino acid in the ligand binding domain of the human androgen receptor (AR) can induce functional abnormalities; for example, in androgen binding or interactions with coregulators. We report here on the structure/function analysis of the AR_{E709K} substitution that is associated with partial androgen insensitivity syndrome. We introduced several mutations at position 709 and tested the consequences of these changes on AR structure and activity in the presence of androgen and antiandrogens. Our results demonstrate that a strong interaction between helix H12 and residue 709 in H3 is required to obtain a fully functional AR. We show that glutamic acid 709 can be replaced by a bulky tyrosine residue without significant effect on the activation by agonists. In contrast, smaller or linear residues that are unable to maintain a tight interaction with H12 induce a substantial loss of androgen-induced AR activity. We also show that the agonist activity of partial antiandrogens is dependent on the side-chain residue at position 709. Strikingly, the AR_{E709Y} substitution causes the conversion of cyproterone acetate into a pure antiandrogen and bicalutamide into a partial agonist. Together, our structural and functional data reveal the key role of glutamic acid 709 in androgenic and antiandrogenic activities. (*Molecular Endocrinology* 20: 724–734, 2006)

NATURAL ANDROGENS, such as testosterone (T) and dihydrotestosterone (DHT), have a critical role in the development, growth and maintenance of the male reproductive system (1). They exert their effect via the intracellular androgen receptor (AR). AR is a member of the nuclear receptor (NR) superfamily, a large family of ligand-activated transcription factors (for a review, see Ref. 2).

First Published Online December 22, 2005

Abbreviations: AF, Activation function; AIS, androgen insensitivity syndrome; AR, androgen receptor; Bmax, maximum androgen binding; CFP, cyan fluorescent protein; CPA, cyproterone acetate; DHT, dihydrotestosterone; ECFP, enhanced CFP; EYFP, enhanced YFP; hAR, human AR; Kd, dissociation constant; LBD, ligand binding domain; MMTV-luc, mouse-mammary-tumor-virus-luciferase; NR, nuclear receptor; PAIS, partial AIS; SDS, sodium dodecyl sulfate; SMRT, silencing mediator of retinoic acid and thyroid hormone receptor; T, testosterone; TIF, transcription intermediary factor; VP16, herpes simplex viral protein 16; wt-AR, wild-type AR; YFP, yellow fluorescent protein.

***Molecular Endocrinology* is published monthly by The Endocrine Society (http://www.endo-society.org), the foremost professional society serving the endocrine community.**

The unliganded AR (apo-receptor) is primarily localized in the cytoplasm. Upon ligand binding (holo-receptor), AR is translocated into the nucleus, moves to different subnuclear sites, binds to specific DNA sequences, and activates androgen-specific genes through protein-protein interactions with coregulatory proteins and general transcription factors. Like other members of the NR superfamily, AR is modular and includes an amino-terminal region containing a ligand-independent transcriptional activation domain [activation function (AF)-1], a central DNA-binding domain that specifically recognizes response elements upstream of target genes, and a carboxy-terminal ligand binding domain (LBD). The LBD is a multifunctional domain, capable of ligand binding, dimerization and interaction with transcriptional coregulators that enhance (coactivators) or decrease (corepressors) the transcriptional activity of the receptor.

The crystal structures of many NR LBDs, including AR, have now been determined, revealing a conserved fold and a common mechanism of activation (3, 4). Upon agonist binding, NR LBDs undergo conformational changes in such a way that some residues belong-

ing to helices H3, H4, and H11 are clustered to form a predominantly hydrophobic surface onto which the apolar side of the highly mobile C-terminal LBD helix H12, encompassing the core of the activation function-2 (AF-2), binds in a stable conformation. In this so-called active- or holo-conformation, helices H3, H4, and H12 define a binding surface that specifically interacts with the LxxLL motifs of coactivators or with the closely related FXXLF motif contained in the amino-terminal (AF-1) domain of AR (5). Binding of antagonists prevents the formation of this specific surface by interfering directly or indirectly with the active conformation of H12.

Mutations in the AR gene can alter the receptor function, which leads to androgen insensitivity syndrome (AIS), a major cause of male pseudohermaphroditism. AIS encompasses a wide spectrum of undervirilization phenotypes ranging from complete AIS in subjects with female phenotype to partial AIS (PAIS) in men with isolated infertility. Mutation of a single amino acid in the AR LBD can lead to abnormalities in androgen binding (6), active conformation stability (7), or interaction with coactivators (8). For example, it has been shown that some AR mutants display altered ligand specificity, resulting in activation of gene transcription upon binding of antiandrogens or other related steroids (9–11). Recently, Hara *et al.* (12) described the W741L mutation that converts the antiandrogen bicalutamide into a partial agonist. This AR gene mutation is thought to contribute to the bicalutamide withdrawal syndrome observed in the treatment of prostate cancer. The characterization of such mutations significantly contributes to our understanding of the structure-function relationships of AR.

Here, we report on a functional and structural study of the AR_{E709K} mutant that we identified in a patient referred in the neonatal period for micropenis (15 mm) and perineoscrotal hypospadias. The same mutation was previously isolated from a patient with a similar PAIS phenotype (13) as well as from a yeast genetic screening (14). We introduced several mutations at position 709 and tested the consequences of these changes on AR structure and activity in the presence of androgens and antiandrogens. These studies allowed us to characterize the functional defects of AR_{E709K} and to provide a molecular rationale for the PAIS phenotype associated with the mutant. Moreover, we demonstrate the key role of glutamic acid 709 in the stabilization of the active conformation of AR and in androgen and antiandrogen activities.

RESULTS

Mutations at Position 709 Affect AR Structure and Functions

We identified a substitution in a patient with PAIS (grade 4 in Quigley's classification; 15) that transforms the amino-acid 709 from a glutamic acid to a lysine. The role of the residue at position 709 in AR LBD helix H3 was investigated by functional studies of the natural (E709K) and artificial (E709A and E709Y) mutants.

After verification by Western blot of expression levels in transfected cells (Fig. 1A), the functional properties of these mutants were evaluated and compared with those of the wild-type receptor (wt-AR). The maximum binding capacities were in the same range for wt-AR and AR variants (Fig. 1B; 558, 614, 507, and 529 fmol/mg protein for wt-AR, AR_{E709K}, AR_{E709A}, and AR_{E709Y}, respectively). The ligand-binding and transactivation properties of the AR_{E709Y} mutant were almost identical to those of wt-AR, with apparent equilibrium binding affinity (Kd) values of 0.25 nM and 0.19 nM (Fig. 1B), respectively, and an EC_{50} of 2.10^{-11} M (Fig. 1D). In contrast, substitution of E709 with lysine or alanine slightly altered the Kd (0.82 and 0.42 nM, respectively) (Fig. 1B), while increasing the dissociation rates of R1881-receptor complexes ($t_{1/2}$ of 25 and 27 min for AR_{E709K} and AR_{E709A}, respectively, *vs.* 60 min for wt-AR) (Fig. 1C). Similarly, the hormone-response curves for transcriptional activity of AR_{E709K} and AR_{E709A} were shifted in EC50 from 2.10^{-11} M to 2.10^{-10} M (Fig. 1D).

To find out whether the decreased transcriptional potency displayed by AR_{E709K} and AR_{E709A} could be correlated with a weakened stability of their active conformations, we analyzed their resistance to limited proteolysis. In the absence of ligand, wt-AR was almost completely degraded by trypsin at a final concentration of 25 μg/ml (Fig. 2). 10^{-8} M R1881 was sufficient to protect the receptor in a 29-kDa resistant fragment previously demonstrated as being characteristic of AR holo-conformation (16). Similarly, all three AR mutants were also digested in the absence of ligand. However, although 10^{-8} M R1881 was sufficient to stabilize AR_{E709Y} in the 29-kDa resistant band, a maximum protection of AR_{E709K} and AR_{E709A} mutants was only obtained with 10^{-6} M R1881.

As shown in Fig. 3A, E709 in helix H3 is solvent-exposed and projects toward helix H12 to form hydrogen bonds with the backbone amides of M894 and M895 (17, 18). Therefore, E709 belongs to the H3/H4/H11 surface and participates in the stabilization of holo-H12. Of note, a similar stabilizing interaction was previously observed in ERα between D351 (homologous to E709 in AR) and the backbone amides of L539 and L540 from H12 (19–23). Our biochemical and functional analyses revealed that losing this interaction by substitution for glutamate by alanine or lysine at amino acid 709 produces AR mutants with altered holo-conformation stability and reduced transcriptional potency. Surprisingly, when E709 was substituted by a tyrosine residue, neither the stability nor the activity of AR was affected, suggesting that at least some H3-H12 stabilizing interactions are restored in this mutant. Indeed, a constructed model of the AR_{E709Y} variant reveals

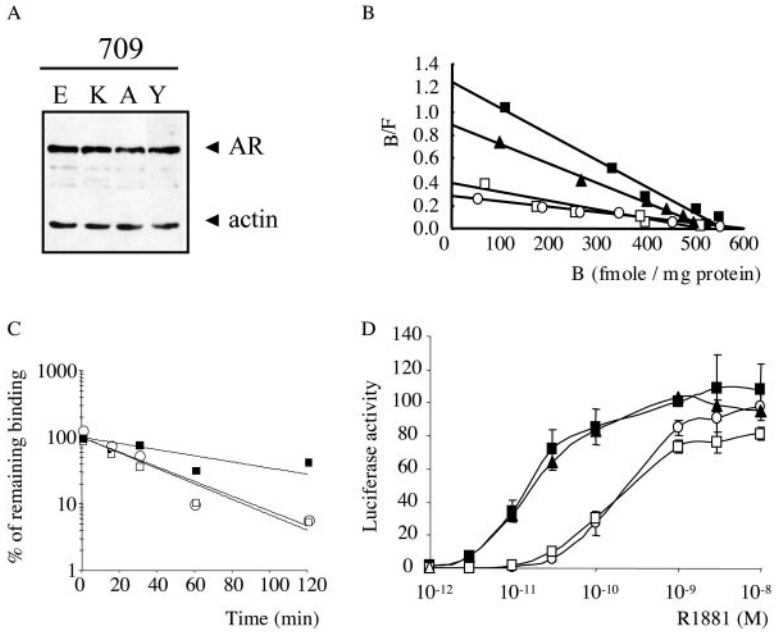

Fig. 1. Expression and Activities of AR Mutants in Transfected Cells

A, Expression levels of different of E709 AR mutants. COS-7 cells were transfected with expression vectors and whole extracts were analyzed by Western blotting using a polyclonal antibody directed against the amino-terminal of AR and a monoclonal antibody against actin. B, Apparent equilibrium binding affinities of AR wild-type and E709 mutants for [^{3}H]R1881 were measured in transfected COS-7 cells. The Kd and the Bmax were derived from Scatchard plots. C, [^{3}H]R1881 dissociation kinetics from wt-AR and E709 mutants by competition with nontritiated R1881. The half-time represents the time required for half dissociation of the bound counts. D, Transcriptional activity of E709 mutants evaluated in CV-1 cells cotransfected with vectors expressing receptors, an androgen-regulated gene (MMTV-luc) and plasmid for β-galactosidase constitutive expression. The cells were incubated in the presence of increasing concentrations of R1881. Luciferase activity detected in cells expressing E709 in the presence of 1 nM R1881 is taken as 100%. These data are the average of four independent experiments (■, wt-AR; ○, AR_{E709K}; □, AR_{E709A}; ▲, AR_{E709Y}). B/F, Bound/free; E, glutamic acid; K, lysine; A, alanine; Y, tyrosine.

that, in opposition to smaller or linear amino acids like alanine or lysine, the bulky tyrosine residue can form improved van der Waals contacts with the side chains of residues P892, E893, M894, and M895 of H12 (3.92 Å, 4.25 Å, 3.77 Å, and 4.12 Å, respectively), thereby stabilizing holo-H12 (Fig. 3B).

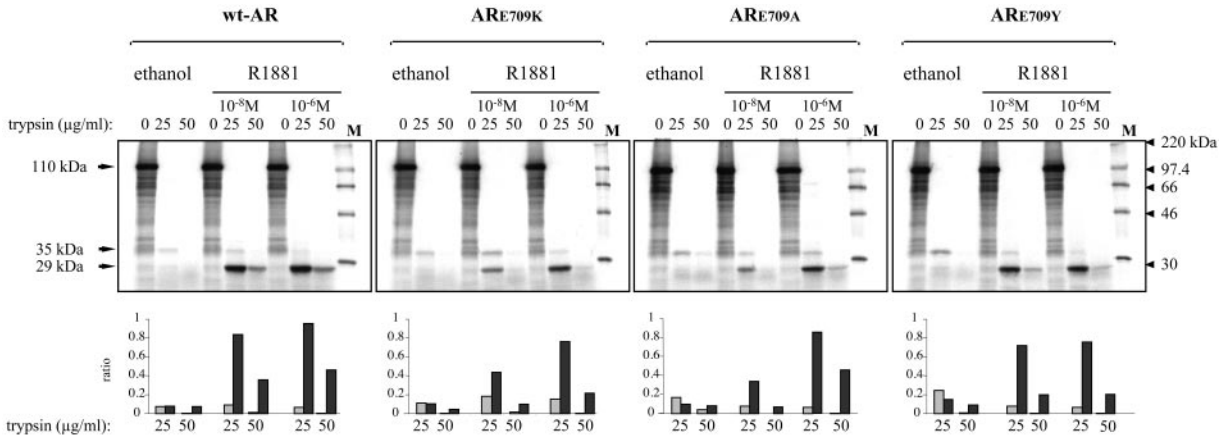

Fig. 2. Agonist-Induced Conformation of AR Mutants

The [^{35}S]-labeled AR was produced in reticulocyte lysate and incubated at 37 C for 30 min with ethanol or R1881 (10^{-8} or 10^{-6} M). The binding product was digested at 27 C by 25 and 50 μg/ml of trypsin. The figure presents the proteolytic resistant fragments separated by 12% SDS polyacrylamide gel and exposed to a Fujix plate for 1 h and to autoradiography overnight. The ^{14}C-labeled protein mass marker (M) migrated as 220-, 97.4-, 66-, 46-, and 30-kDa bands. On the *lower panel*, the relative intensities are represented for 25- and 50-μg/ml concentrations of trypsin: the *gray bar* corresponds to the 35-kDa band (ratio of the 35-kDa band to the 110-kDa band), and the *dark bar* corresponds to the 29-kDa band (ratio of the 29-kDa band to the 110-kDa band).

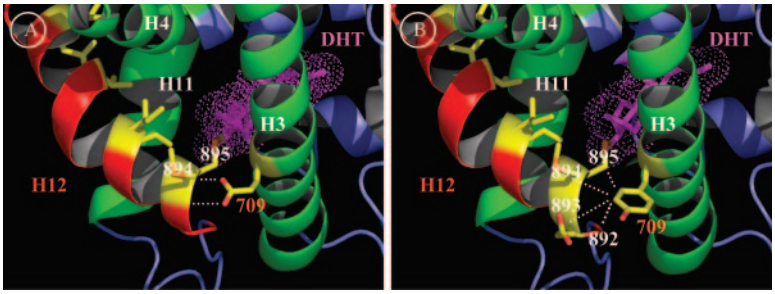

Fig. 3. Stabilization of the Active AR Conformation by Interactions between H3 and holo-H12

A. Close-up view of the coactivator binding site of AR LBD (PDB ID code 1I37). When bound to an agonist (DHT), helix H12 is stabilized against H3, H4, and H11. This conformation corresponds to the active form of the receptor because it generates a specific surface containing residues from H3, H4, and H12 onto which coactivators can bind. The figure shows the stabilizing interaction between E709 of H3 and M894 and M895 from H12. B, Same view of a constructed model of the AR_{E709Y} mutant showing the predicted van der Waals interactions between Y709 and some H12 residues. Helices H3, H4, and H11 are labeled and represented as *green ribbons*. The activation helix H12 is shown in *red*. H12 hydrophobic residues mediating the interaction with the LBD core as well as residues at position 709 are represented as *thick lines* (carbon, *yellow*; oxygen, *red*). The bound ligand (DHT) is in *magenta*.

Together, these results demonstrate that the interaction between the residue at position 709 and helix H12 is critical for both ligand-binding and receptor activation by stabilizing the holo-conformation of AR.

Mutations at Position 709 Convert Cyproterone Acetate to a Pure Antiandrogen and Bicalutamide to a Partial Antiandrogen

We investigated the agonist and antagonist properties of antiandrogens on the various AR constructs. In this study, we used steroidal (cyproterone acetate; CPA) and nonsteroidal (hydroxyflutamide, nilutamide, and bicalutamide) antiandrogens (Fig. 4). Antagonist activities were measured by using increasing concentrations of antiandrogen in competition with a constant R1881 concentration. The R1881 concentration used in each experiment was proportional to the EC_{50} obtained in R1881-induced transcriptional activity (10^{-10} M R1881 for wt-AR and AR_{E709Y}, and 10^{-9} M R1881 for AR_{E709K} and AR_{E709A}).

As shown in Fig. 4, whereas CPA displayed partial agonist activity on wt-AR, it exhibited almost no activity on either mutant. Accordingly, 10^{-6} M CPA only partially reduced the transcriptional activity of wt-AR induced by R1881, whereas it drastically inhibited the R1881-dependent activity of the AR mutants. CPA inhibited the androgen-induced wt-AR activity at lower concentrations than those required with AR_{E709Y}, revealing a decreased affinity of CPA for this variant. Except with hydroxyflutamide at very high concentration, none of the mutations affected the androgenic or antiandrogenic profile of hydroxyflutamide or nilutamide (Fig. 4). Interestingly, whereas the AR_{E709K} and AR_{E709A} mutations did not significantly affect the agonist properties of bicalutamide (Fig. 4), the AR_{E709Y} mutant displayed an increased transcriptional activity in response to this antiandrogen, which reached 55% of maximal transactivation. Accordingly, bicalutamide inhibited the R1881-induced luciferase activity of AR_{E709K} and AR_{E709A} as efficiently as that of wt-AR, whereas only a partial deactivation of AR_{E709Y} was obtained. Moreover, bicalutamide inhibited the R1881-induced activity at the lowest concentration used (10^{-8} M), indicating an increased affinity of bicalutamide for AR_{E709Y}. These data clearly demonstrate that mutations E709K and E709A abolish the agonist activity of antiandrogens, thereby increasing their antagonist potential, and that substitution of E709 by a tyrosine transforms CPA from a partial antagonist into a pure antiandrogen, and bicalutamide from a pure antiandrogen into a partial agonist.

To evaluate the impact of mutations at position 709 on the antagonist-induced AR conformations, we performed limited proteolysis assays (Fig. 5). In line with its partial androgenic character, 10^{-7} M CPA stabilized wt-AR in a conformation providing a major 35-kDa resistant form reported to correspond to a receptor inactive conformation (16), whereas a clear 29-kDa band characteristic of the active AR conformation appeared at higher CPA concentration. Proteolytic digestion of wt-AR incubated with the antiandrogens hydroxyflutamide, bicalutamide or nilutamide resulted in a unique 35-kDa-resistant fragment. In full agreement with our functional data, we observed that all three AR mutants were protected in a major 35-kDa fragment in the presence of 10^{-7} M and 10^{-5} M CPA, hydroxyflutamide, and nilutamide. Bicalutamide stabilized AR_{E709K} and AR_{E709A} in an inactive conformation providing a 35-kDa-resistant fragment, whereas a clear additional 29-kDa band appeared with AR_{E709Y}. The simultaneous presence of the two resistant fragments suggests that helix H12 of AR_{E709Y} is in equilibrium between the inactive and active conformations in the presence of bicalutamide.

This analysis reveals that mutations of E709 modify the antiandrogenic profile of CPA and bicalutamide. Strikingly, the E709Y mutation transforms CPA into a

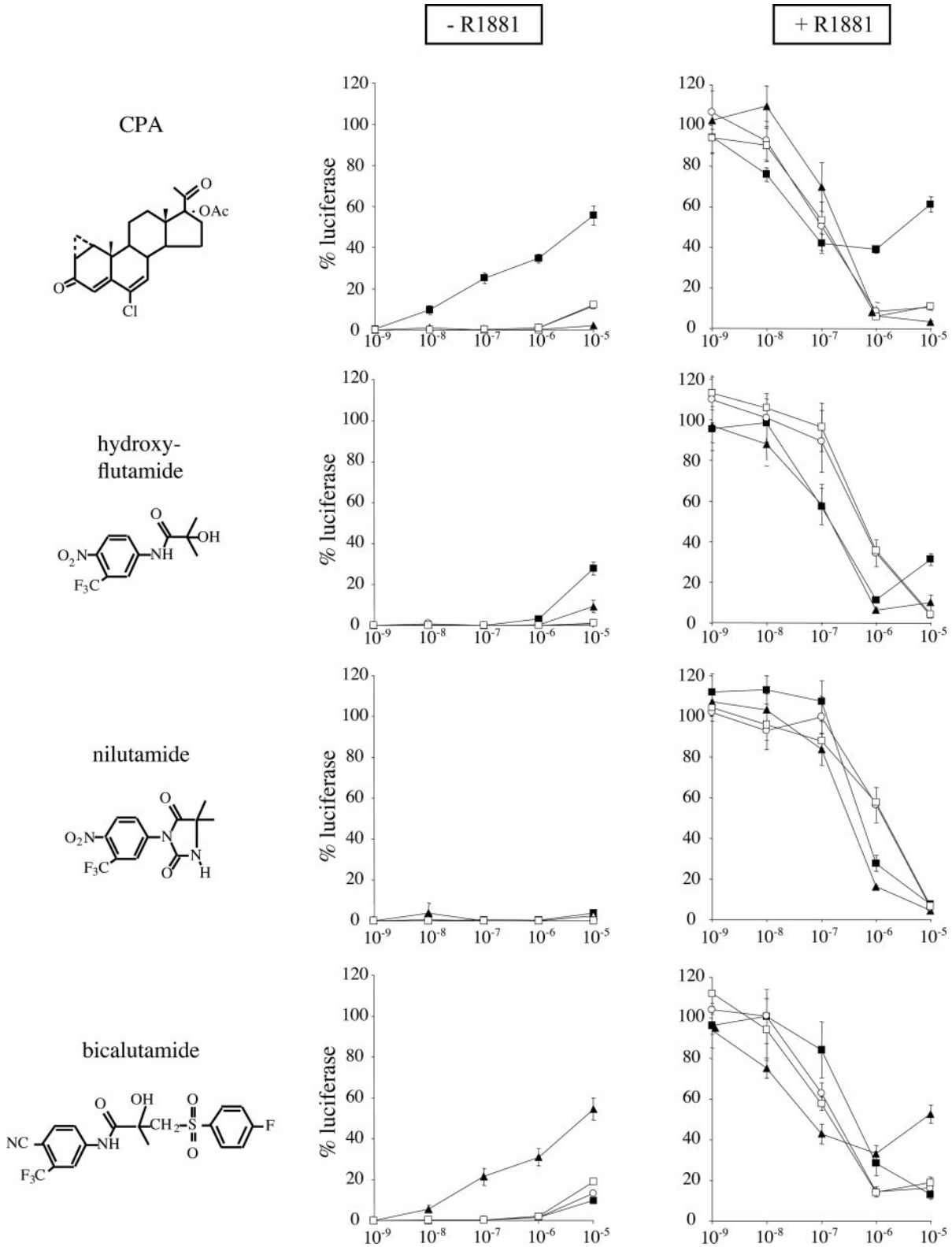

Fig. 4. Agonist and Antagonist Effects of Antiandrogens on Transcriptional Activities of AR Mutants

CV-1 cells transfected with AR expression vectors and androgen-dependent reporter gene (MMTV-luc) were incubated in the presence of increasing concentrations of antiandrogen alone or in competition with 10^{-10} M R1881 for wt-AR and AR_{E709Y}, and with 10^{-9} M R1881for AR_{E709A} and AR_{E709K}. Luciferase activities were measured in all these conditions and expressed as a function of R1881 activity for each receptor taken as 100%. These data are the averages of four independent experiments (■, wt-AR; ○, AR_{E709K}; □, AR_{E709A}; ▲, AR_{E709Y}).

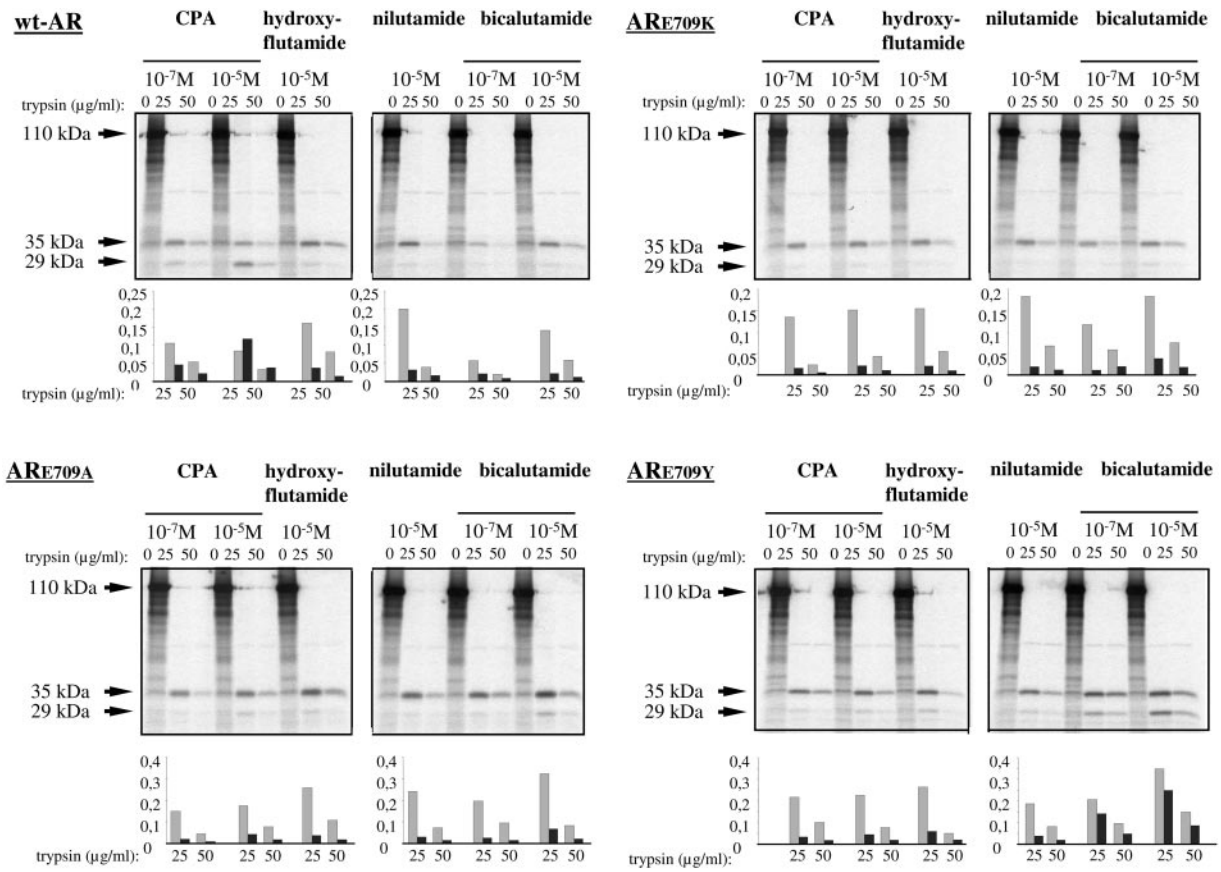

Fig. 5. Antiandrogen-Induced Conformational Changes of ARE709 Mutants

The incubations of *in vitro*-produced wt-AR and mutated AR with CPA (10^{-7} M and 10^{-5} M), hydroxyflutamide (10^{-5} M), bicalutamide (10^{-7} M and 10^{-5} M), and nilutamide (10^{-5} M) were followed by a treatment at 27 C with trypsin (25 and 50 μg/ml) for 10 min. Trypsin-digested products were separated by SDS-PAGE and visualized by autoradiography. On the *lower panel*, the relative intensities are represented for each concentration of the trypsin lanes: the *gray bar* corresponds to the 35-kDa band (ratio of the 35-kDa band to the 110-kDa band) and the *dark bar* corresponds to the 29-kDa band (ratio of the 29-kDa band to the 110-kDa band).

pure antagonist by shifting the conformational equilibrium of the AR_{E709Y}/CPA complex toward the inactive conformation. Inversely, the same mutation allows the AR_{E709Y}/bicalutamide complex to transiently adopt the active conformation, thereby converting bicalutamide into a partial agonist.

Coactivator and Corepressor Interactions with wt-AR and AR_{E709Y}

Paralleling our observations, it has been previously reported that the mutation homologous to AR_{E709Y} in ERα ($ER\alpha_{D351Y}$) changes the pharmacology of raloxifene or tamoxifen by shifting their antiestrogenic activity to an estrogenic activity (19–23). Whereas tamoxifen promotes association between wt-ERα and corepressors, Yamamoto *et al.* (24) reported that $ER\alpha_{D351Y}$ exhibits a reduced tamoxifen-induced interaction with nuclear receptor corepressor/silencing mediator of retinoic acid and thyroid hormone receptor (SMRT) and consequently a high tamoxifen-induced AF-1 activity. Therefore, to determine whether the partial agonistic activity of bicalutamide, in the context of AR_{E709Y}, is due to a gain of coactivator interaction or a loss of corepressor binding, we analyzed the coregulator recruitment by wt-AR and AR_{E709Y} in the presence of CPA and bicalutamide. Interactions of wt-AR and AR_{E709Y} with the corepressor SMRT (25) or the coactivactor transcription intermediary factor 2 (TIF2) (a member of the p160 family of coactivators; 26) were monitored using a modified mammalian two-hybrid system. In this assay, interaction between full-length AR and the VP16 (herpes simplex viral protein 16) fusions of the interacting domains of TIF2 (TIF2-ID) and SMRT (SMRT-ID) leads to an increase in luciferase gene expression. Figure 6 shows that both SMRT-ID and TIF2-ID interacted with R1881-bound wt-AR and AR_{E709Y} with, however, a 10-fold stronger two-hybrid signal obtained with the coactivator. None of the antihormones tested promoted a significant interaction between SMRT-ID and wt-AR or AR_{E709Y}. When wt-AR was cotransfected with TIF2-ID, a partial CPA-

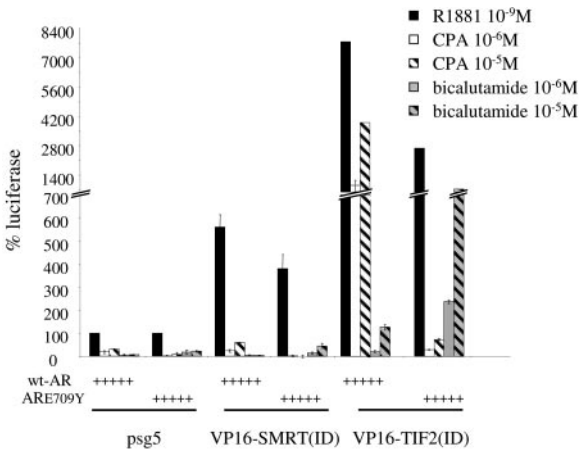

Fig. 6. Ligand-Induced Cofactor-AR Interaction

Modified mammalian two-hybrid experiment in which full-length wt-AR or AR_{E709Y} mutant, MMTV-luc reporter and the expression plasmid coding for VP16-TIF2 or VP16-SMRT (fusion proteins between the interaction domain of TIF2 or SMRT with the VP16 activation domain) were cotransfected. Cells were stimulated by 10^{-9} M R1881 (*black bar*), 10^{-6} M CPA (*open bar*) and 10^{-5} M (*hatched bar*) and bicalutamide 10^{-6} M (*gray bar*) and 10^{-5} M (*hatched gray bar*). Transcriptional activities were expressed as luciferase activity relative to luciferase activity obtained for E709 and E709Y with 10^{-9} M R1881 in the absence of VP16-cofactor and taken as 100%.

induced luciferase activity was obtained. In contrast, the partial agonist activity of CPA was almost completely abolished when using AR_{E709Y}. Conversely, bicalutamide was able to induce a clear interaction of TIF2-ID with AR_{E709Y} but not with wt-AR.

To further characterize AR-TIF2 interaction *in vivo*, we cotransfected wt-AR or AR_{E709Y} and TIF2 fused to variants of green fluorescent protein [ECFP, enhanced CFP (cyan fluorescent protein) and EYFP, enhanced YFP (yellow fluorescent protein), respectively] and analyzed their subcellular localization by double fluorescence observation. Cells were stimulated with R1881, CPA, or bicalutamide for 8 h, fixed, and observed with a confocal fluorescence microscope. The redistribution of TIF2 from nuclear foci to the nucleoplasm by the agonist-bound AR has been described by several laboratories (27, 28). Figure 7 shows that TIF2 redistribution was observed when wt-AR was coexpressed in the presence of R1881 or CPA. Wt-AR complexed to bicalutamide failed to recruit TIF2 in the nucleoplasm because there was no coactivator redistribution (Fig. 7). AR_{E709Y} redistributed TIF2 after addition of R1881 or bicalutamide, whereas CPA treatment did not affect TIF2 localization in the nuclear foci.

Altogether, these data show that the modified functional activity of CPA and bicalutamide can be explained by a decreased recruitment of coactivator by AR_{E709Y} in the presence of CPA and an increased recruitment of coactivator in the presence of bicalutamide. In contrast to $ER\alpha_{D351Y}$, the interaction between AR_{E709Y} and SMRT-ID in the presence of CPA or bicalutamide remains unchanged relative to wt-AR.

DISCUSSION

The cumulative data from previous studies indicate that the regulation of the transcriptional activity of NRs by their ligands depends on the modulation of the

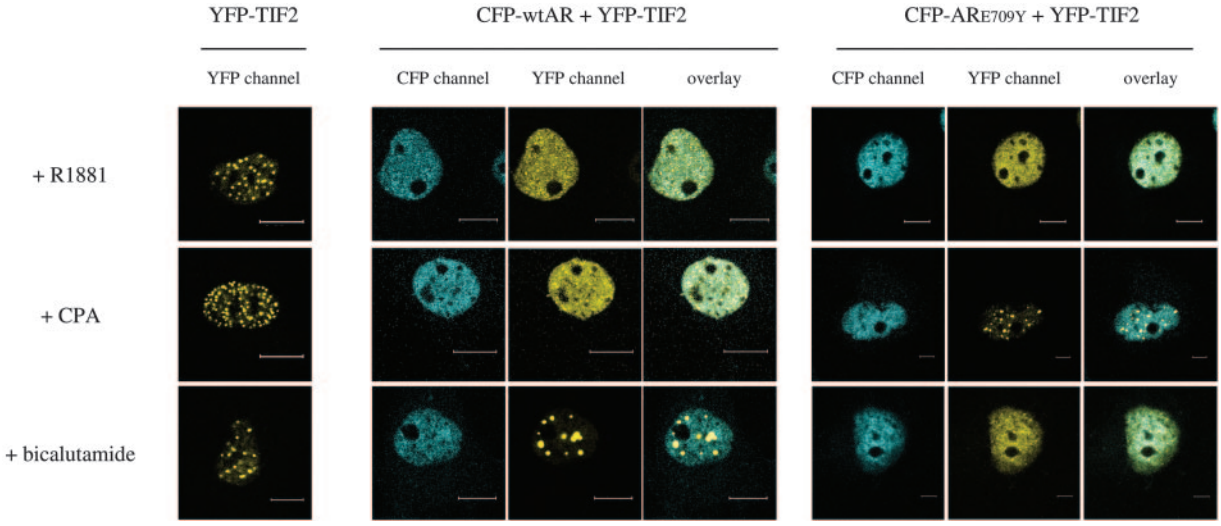

Fig. 7. Ligand-Induced Intranuclear Distribution of CFP-AR and YFP-TIF2

COS-7 cells were transiently transfected with vectors expressing fusion proteins YFP-TIF2 alone or combined to CFP-wt-AR or CFP-AR_{E709Y}. Cells were incubated in the presence of ligands (10^{-9} M R1881, 10^{-6} M CPA and bicalutamide) for 8 h, fixed with 4% paraformaldehyde and observed using a Leica SP2 Confocal microscope. Images were analyzed with Leica software and merged images were generated by Adobe Photoshop software (*scale bar*, 4 μm). Pseudocolors were used (*blue* for CFP and *yellow* for YFP).

dynamic properties of the most C-terminal LBD activation helix H12 (29). In this paper, we report on the role of glutamic acid at position 709 of AR in the stabilization of helix H12 in the active conformation.

Our biochemical and functional experiments demonstrate that the AR_{E709K} and AR_{E709A} mutations destabilize the AR-androgen complex with an increased dissociation rate and a lower protection from trypsic digestion. This structural instability explains the partial transactivation capacities exhibited by these mutants bound to the agonist R1881. Yeh *et al.* (13) previously described the AR_{E709K} mutation in a patient with PAIS. Their *in vitro* studies suggested that this AR mutant displays only a slightly reduced DHT-mediated AR activity, with, however, a single concentration of DHT tested (13, 30). The authors explored the response of AR to estrogens and proposed that the consequence of losing the estradiol-AR_{E709K}-ARA70 pathway while maintaining the DHT-AR_{E709K}-ARA70 pathway might likely be one of the explanations for the observed PAIS (13). The deficiency of androgen action that we describe in the present report appears more relevant to explain this PAIS phenotype with respect to what is known of androgen action for sex differentiation. Surprisingly, our data show that mutation of E709 by a tyrosine has no significant effect on the transcriptional activity and coactivator recruitment of androgen-bound AR. Molecular modeling and conformational studies suggest that van der Waals contacts between Y709 and some side-chain residues of H12 might help to stabilize the active conformation of the AR_{E709Y}/agonist complex, whereas the stabilizing interactions between holo-H12 and E709 are completely abolished in the AR_{E709K} and AR_{E709A} mutants.

We next examined the contribution of glutamic acid 709 to the antagonist activity of several partial and full antiandrogens. We first substantiated the partial agonist/antagonist character of CPA, which appears unable to fully stabilize the proper H3/H4/H11 surface required for holo-H12 positioning. Indeed, the weak androgenic activity displayed by CPA and the proteolytic digestion pattern showing the simultaneous presence of the 29- and 35-kDa-resistant bands suggest that AR can adopt both active and inactive conformations when bound to CPA. Therefore, in contrast to pure antagonists like hydroxyflutamide, bicalutamide, or nilutamide that almost completely abrogate the active conformation of AR LBD, CPA allows the active conformation of H12 to be reached transiently, thereby accounting for its partial androgenic activity.

All the 709 AR mutations tested abrogated the residual androgenic activity displayed by CPA. The drastic effect of the mutations on the activation profile of CPA can be simply explained by the fact that the binding of a full agonist like DHT or R1881 induces the optimal H3/H4/H11 surface, offering maximum productive interactions between the LBD core and holo-H12, whereas only a subset of these interactions is generated in the presence of CPA. In consequence, whereas in the AR/R1881 complex the presence of E709 is not absolutely required for at least partial AR activation, the substitution of this residue completely abolishes the residual androgenic activity of CPA because the few remaining van der Waals contacts between H12 and the LBD core cannot compensate for the loss of interaction between E709 and holo-H12.

None of the mutations tested had a significant effect on the antiandrogenic profile of hydroxyflutamide or nilutamide. In contrast, the E709Y mutation transformed the antiandrogen bicalutamide into a partial agonist. To support this finding, we provided experimental evidence that the replacement of E709 by a tyrosine allows bicalutamide to induce AR active conformation and its interaction with coactivators. Due to the poor structural homology between steroidal and nonsteroidal ligands, no attempt was made to build a model for the antagonist-bound AR LBD. However, because of the modest molecular size of hydroxyflutamide and nilutamide and because they lack a bulky side chain, it is very likely that these ligands antagonize AR through the molecular mechanism previously described as passive antagonism (31). Conversely, due to its larger size, it is unlikely that bicalutamide can be contained within the agonist-binding cavity of AR. The x-ray structure of the AR_{W741L} LBD mutant bound to bicalutamide was recently reported (32). This mutation confers agonist activity to bicalutamide (33) and, indeed, an active (holo) conformation of the AR_{W741L}/bicalutamide complex was observed in the crystal. Although the structure does not provide direct experimental information on the structural antagonist mechanism of bicalutamide, it demonstrates that the sulfonyl-linked phenyl ring (B-ring) of the antiandrogen is accommodated at the location of the indole ring of W741 in wt-AR. Therefore, in wt-AR, the B-ring of bicalutamide probably protrudes out of the opening to the binding pocket between helices H3 and H11, thereby preventing H12 from adopting the active conformation. The gain in androgenic activity of bicalutamide in the context of AR_{E709Y} is difficult to reconcile convincingly on the basis of our current structural knowledge. Further structural work will be required to understand how bicalutamide can stabilize the holo-conformation of AR_{E709Y} and how the mutation increases the affinity of bicalutamide for the receptor.

In conclusion, we analyzed the functional role of E709 in helix H3 of AR LBD. We provide evidence that the H3/H12 interaction mediated by E709 is required for optimal androgen-dependent coactivator recruitment and transcriptional activation. Furthermore, the relative agonist *vs.* antagonist activity of antiandrogens is highly dependent on the side-chain residue at position 709. Our data show that the mutation of E709 to tyrosine suffices to abolish the androgenic activity of CPA and to transform bicalutamide into a partial androgen. Both our structural and functional data reveal the key role of glutamic acid 709 for androgenic and antiandrogenic activities.

MATERIALS AND METHODS

Patient

The patient was referred for ambiguous genitalia in the neonatal period. The parents were not related, and there was no family history of similar cases. Genital examination revealed a micropenis (15 mm) with perineoscrotal hypospadias. The two testes were palpable within labioscrotal folds. The basal testosterone value from 16.7 nM at 6 wk of age and increased to 38.0 nM after the human chorionic gonadotropin stimulation test. Male sex of rearing was chosen.

Direct Sequencing of Patient DNA

DNA was extracted from peripheral blood leukocytes. The eight exons and flanking intron regions of the human AR gene were screened for mutations by direct sequencing of the amplified PCR products, using sets of primers previously described (34) and an ABI Prism Big Dye Terminator Sequencing kit (Applied Biosystems, Courtaboeuf, France). The sequencing reactions were analyzed on a ABI 310 genetic analyzer.

Construction of the Variant AR cDNA Expression Vectors

To obtain the natural mutant vector (AR_{E709K}), a *Kpn*I-*Bam*HI fragment (containing both DNA- and androgen-binding domains) was cleaved from pSG5-human AR (hAR) and subcloned into the corresponding site of pUC19 (pUC19-hAR). The amplified fragment of the patient's exon 4 was digested by Tth 111-I and *Stu*I, and the purified fragment was ligated to pUC19-hAR, whose normal Tth 111-I and *Stu*I fragment was previously cleaved. Finally, the mutated exon 4 cloned into the *Kpn*I-*Bam*HI fragment was inserted into the corresponding sites of pSG5-hAR to yield pSG5-hAR-E709K, the expression vector of mutated AR.

Artificial E709A and E709Y mutants were obtained in AR cDNA in pSG5-hAR by site-directed mutagenesis (Stratagene, La Jolla, CA) using PCR amplification with specific primer containing mutation, and digestion of parental DNA with *Dpn*I according to the manufacturer's procedures. The primers used were:

5′-GCCTCAATGAACTGGGAGCGAGACAGCTTGTACACGTGG-3′ for E709A, 5′-GCCTCAATGAACTGGGATATCGACAGCTTGTACACGTGG-3′ for E709Y, and the complementary sequences for antisense primers. Amplified and *Dpn*I digested products were directly transformed into *Escherichia coli* DH5α (Life Technologies, Cergy, France). Different clones were amplified and the extracted DNA was sequenced to verify the mutation insertion.

The plasmid pECFP-AR was obtained by insertion of AR excised by the *Nhe*I and *Bgl*II restriction sites from pGFP-AR, as previously described (35), into pECFP-C1 (CLONTECH, Palo Alto, CA). pECFP-AR_{E709Y} was constructed by exchange of the *Kpn*I-*Pvu*I fragment from pSG5-hAR-E709Y containing the mutation with the identical fragment into pECFP-wt-AR. pEYFP-TIF2 was produced by insertion of TIF2 cDNA amplified by PCR from psg5-TIF2 into pcDNA3-EYFP by *Kpn*I and *Eco*RI cloning sites. All amplifications were performed in *E. coli* DH5α, and all steps were verified by sequencing.

Coupled *in Vitro* Transcription and Translation

Expression plasmids (pSG5-hAR wild-type or mutants) were transcribed and translated with the TNT T7 Quick Coupled Transcription/Translation System (Promega, Charbonnieres, France) in the presence of [^{35}S]methionine (1000 Ci/mmol; Amersham, Orsay, France), according to the manufacturer's instruction, for 2 h at 30 C.

Limited Proteolysis Assays

Five microliters of [^{35}S]-receptor synthesized *in vitro* were preincubated at 37 C for 30 min with 0.5 μl of vehicle or ligand. Limited proteolysis was performed by the addition of 5 μl of various trypsin amounts (0, 25, and 50 μg/ml; final concentration). Incubations with protease were conducted at 27 C for 10 min and stopped by the addition of 10 μl of sodium dodecyl sulfate (SDS) sample buffer and chilling on ice. The samples were boiled for 5 min. The products of proteolysis were separated on a 0.75-mm-thick, 12% SDS polyacrylamide gel. After electrophoresis, the gels were washed in distilled water and vacuum-dried for 20 min. Gels were exposed to a Fujix (Tokyo, Japan) film imaging plate for 1 h and to autoradiography overnight. Band intensity was semiquantified with Fujix software.

Cell Culture

COS-7 cells and CV-1 cells were cultured in DMEM (Life Technologies) supplemented with 10% fetal calf serum, penicillin (100 U/ml) and streptomycin (100 μg/ml) in a humidified atmosphere containing 5% CO_2. Cells were transiently transfected using the calcium phosphate DNA precipitation method. After overnight incubation, precipitates were removed and replaced by fresh DMEM without fetal calf serum.

Immunoblot

In 100-mm dishes, COS-7 cells (10^9 cells) were transfected with 10 μg of pSG5-hAR wt or mutants. Forty-four hours later, cells were lysed directly in the dish with 50 μl of lysis buffer [40 mM Tris (pH 7.4), 1 mM EDTA, 10% glycerol, 1% Triton X-100, 0.5% sodium deoxycholate, and 0.08% SDS] supplemented with a cocktail of protease inhibitors (Sigma, Saint Quentin Fallavier, France). The cellular debris was pelleted at 13,000 $\times$ *g* for 10 min and the protein concentration was determined on a supernatant aliquot by the Lowry quantification method. The lysate was mixed vol/vol with SDS sample buffer and boiled for 10 min. The total proteins (50 μg) of each extract were subjected to 10% SDS-PAGE and Western transfer by electroblotting. Nitrocellulose filters were saturated in TBS [20 mM Tris-HCl (pH 7.4), 500 mM NaCl] plus 10% milk and 0.05% Tween 20 at room temperature. Filters were then incubated with polyclonal anti-AR antibody (SpO61) diluted 1/2000 (36) and antiactin (Sigma) diluted 1/2000, followed by hybridation of peroxidase-conjugated antirabbit IgG diluted 1/5000 (Amersham). Blots were developed using the ECL chemiluminescent detection system (Pierce, Rockford, IL).

Androgen-Binding and Dissociation Assays

To determine the binding characteristics of the hAR mutants compared with the wild-type receptor, COS-7 cells were transiently transfected in 12-well dishes with 50 ng of pSG5-hAR wild-type or mutant and 250 ng of pCMV-β-galactosidase. After 48 h at 37 C, the transfected cells were incubated at 37 C for 2 h with increasing concentrations (0.05–4 nM) of [^{3}H]R1881 for total binding. Nonspecific binding was measured in parallel incubations containing an additional 1000-fold molar excess of radioinert ligand. In parallel, the dissociation rate of the R1881-receptor complex in COS-7 cells was measured in transfected cells by incubation with 4 nM of [^{3}H]R1881 at 37 C for 2 h, followed by the addition of a 1000-fold excess of unlabeled ligand for various times. Nonspecific binding was determined from cells that were treated

with 4 nM [^{3}H]R1881 in the presence of a 1000-fold excess of unlabeled R1881.

The cells were harvested in lysis buffer: 25 mM Tris-H_3PO_4 (pH 7.8), 2 mM dithiothreitol, 2 mM EDTA, 1% Triton X-100, and 10% glycerol. Aliquots were used for radioactivity measurement, β-galactosidase activity, and protein assay. After subtraction of nonspecific from total binding, the dissociation constants (Kd) and the maximum androgen-binding sites (Bmax) were derived from Scatchard plots, and the percentage of remaining basal R1881-binding was plotted semilogarithmically against time.

Transfection and Luciferase Activity Assay

CV-1 cells or COS-7 cells were transiently transfected in 12-well dishes with 50 ng of pSG5-hAR, 250 ng of pCMV-β-galactosidase to correct for transfection efficiency, and 0.5 μg of p-mouse-mammary-tumor-virus-luciferase (MMTV-luc). For the modified mammalian two-hybrid experiments, 0.5 μg of psg5-, -VP16-TIF2 (interaction domain) or -VP16-SMRT (interaction domain) was added. Precipitate was removed after 16 h and cells were maintained in DMEM with vehicle alone or various ligand concentrations. After 30 h, the cells were lysed by 300 μl of the lysis buffer described above. Luciferase activity was measured by the reaction of lysate with luciferin solution: 270 μM coenzyme A, 470 μM luciferin, 530 μM ATP, 20 mM Tricine (pH 7.8), 1.07 mM $(MgCO_3)_4$ $Mg(OH)_2$ $5H_2O$, 2.67 mM $MgSO_4$ and 1 mM EDTA. Luciferase activity was measured on a centro LB960 luminometer (Berthold, Thoiry, France). Each incubation was performed in duplicate. β-Galactosidase activity was determined to control the efficiency of each transfection. The presented results are the averages of three independent experiments.

Microscopy and Imaging Analysis

COS-7 cells were cultured on coverslips and then transfected with 1 μg of plasmids using 3 μl/dish of Fugene reagent (Roche, Meylan, France). Twenty-four hours after transfection, the culture medium was replaced with serum-free DMEM for overnight starvation. Cells were incubated with R1881 (10^{-8} M) or antihormones (10^{-6} M) for 8 h, fixed with 4% paraformaldehyde for 15 min, washed three times with PBS and mounted on slides with Dako (Carpinteria, CA) mounting medium. The cells were imaged using confocal laser scanning microscopy (Leica SP2 UV system; Leica Microsystems, Heidelberg, Germany). The cells were imaged for cyan fluorescence by excitation with the 457-nm line from an argon laser, and emission was viewed through a 460- to 490-nm band pass filter. The yellow fluorescence was scanned using the 514-nm excitation line and the 520- to 550-nm band pass filter as emission filter.

Receptor Modeling

The AR_{E709Y} LBD model was generated from the AR/DHT crystal structure (18). The E709Y substitution was incorporated using the program O (37) and a conjugate gradient energy minimization was performed with CNS (38). To avoid deviations of the LBD fold during minimization, a harmonic restraint of 10 kcal/Å^2 was applied to all main-chain atoms and crystallographic symmetry-related molecules were incorporated.

Acknowledgments

We thank Dr. H. Richard-Foy (Laboratoire de Biologie Moléculaires des Eucaryotes, Toulouse, France) for providing p-MMTV-luc reporter gene and Dr. H. Gronemeyer (Institut de Génétique et de Biologie Moléculaire et Cellulaire, Strasbourg, France) for providing psg5-TIF2, psg5-VP16-TIF2 and psg5-VP16-SMRT.

Received October 21, 2005. Accepted December 13, 2005.

Address all correspondence and requests for reprints to: Dr. Jean-Claude Nicolas, Institut National de la Santé et de la Recherche Médicale, Unité 540, Endocrinologie Moléculaire et Cellulaire des Cancers, 60 rue de Navacelles, 34090 Montpellier, France. E-mail: nicolas@montp.inserm.fr.

Present address for V.G.: Plateforme Imagerie Cellulaire de l'IFR83, Université Pierre et Marie Curie, Batiment A-4^{e}étage-case 25, 7–9 quai Saint-Bernard, 75252 Paris cedex 05, France.

Present address for S.L.: Laboratoire de Biochimie, Hôpital Carémeau, Centre Hospitalier Universitaire, Nîmes 30000, France.

Potential conflicts of interest: Authors have nothing to declare.

REFERENCES

1. Quigley CA, Debellis A, Marschke KB, Elawady MK, Wilson EM, French FS 1995 Androgen receptor defects: historical, clinical, and molecular perspectives. Endocr Rev 16:271–321
2. Mangelsdorf D, Thummel C, Beato M, Herrlich P, Schütz G, Umesono K, Blumberg B, Kastner P, Mark M, Chambon P, Evans RM 1995 The nuclear receptor superfamily: the second decade. Cell 83:835–839
3. Bourguet W, Germain P, Gronemeyer H 2000 Nuclear receptor ligand-binding domains: three-dimensional structures, molecular interactions and pharmacological implications. Trends Pharmacol Sci 21:381–388
4. Moras D, Gronemeyer H 1998 The nuclear receptor ligand-binding domain: structure and function. Curr Opin Cell Biol 10:384–391
5. Dubbink HJ, Hersmus R, Verma CS, van der Korput HA, Berrevoets CA, van Tol J, Ziel-van der Made AC, Brinkmann AO, Pike AC, Trapman J 2004 Distinct recognition modes of FXXLF and LXXLL motifs by the androgen receptor. Mol Endocrinol 18:2132–2150
6. Sultan C, Lumbroso S, Paris F, Jeandel C, Terouanne B, Belon C, Audran F, Poujol N, Georget V, Gobinet J, Jalaguier S, Auzou G, Nicolas JC 2002 Disorders of androgen action. Semin Reprod Med 20:217–228
7. Lumbroso S, Wagschal A, Bourguet W, Georget V, Mazen I, Servant N, Audran F, Sultan C, Auzou G 2004 A new mutation of the androgen receptor, P817A, causing partial androgen insensitivity syndrome: *in vitro* and structural analysis. J Mol Endocrinol 32:679–687
8. Alen P, Claessens F, Verhoeven G, Rombauts W, Peeters B 1999 The androgen receptor amino-terminal domain plays a key role in p160 coactivator-stimulated gene transcription. Mol Cell Biol 19:6085–6097
9. Veldscholte J, Berrevoets CA, Mulder E 1994 Studies on the human prostatic cancer cell line LNCaP. J Steroid Biochem Mol Biol 49:341–346
10. Warriar N, Page N, Koutsilieris M, Govindan MV 1994 Antiandrogens inhibit human androgen receptor-dependent gene transcription activation in the human prostate cancer cells LNCaP. Prostate 24:176–186
11. Poujol N, Wurtz JM, Tahiri B, Lumbroso S, Nicolas JC, Moras D, Sultan C 2000 Specific recognition of androgens by their nuclear receptor. A structure-function study. J Biol Chem 275:24022–24031
12. Hara T, Miyazaki J, Araki H, Yamaoka M, Kanzaki N, Kusaka M, Miyamoto M 2003 Novel mutations of andro-

gen receptor: a possible mechanism of bicalutamide withdrawal syndrome. Cancer Res 63:149–153
13. Yeh S, Miyamoto H, Shima H, Chang C 1998 From estrogen to androgen receptor: a new pathway for sex hormones in prostate. Proc Natl Acad Sci USA 95: 5527–5532
14. Wang C, Young WJ, Chang C 2000 Isolation and characterization of the androgen receptor mutants with divergent transcriptional activity in response to hydroxyflutamide. Endocrine 12:69–76
15. Quigley CA, De Bellis A, Marschke KB, el-Awady MK, Wilson EM, French FS 1995 Androgen receptor defects: historical, clinical, and molecular perspectives. Endocr Rev 16:271–321
16. Kuil CW, Berrevoets CA, Mulder E 1995 Ligand-induced conformational alterations of the androgen receptor analyzed by limited trypsinization. J Biol Chem 270: 27569–27576
17. Matias PM, Donner P, Coelho R, Thomaz M, Peixoto C, Macedo S, Otto N, Joschko S, Scholz P, Wegg A, Basler S, Schafer M, Egner U, Carrondo MA 2000 Structural evidence for ligand specificity in the binding domain of the human androgen receptor. Implications for pathogenic gene mutations. J Biol Chem 275:26164–26171
18. Sack JS, Kish KF, Wang C, Attar RM, Kiefer SE, An Y, Wu GY, Scheffler JE, Salvati ME, Krystek Jr SR, Weinmann R, Einspahr HM 2001 Crystallographic structures of the ligand-binding domains of the androgen receptor and its T877A mutant complexed with the natural agonist dihydrotestosterone. Proc Natl Acad Sci USA 98:4904–4909
19. Anghel SI, Perly V, Melancon G, Barsalou A, Chagnon S, Rosenauer A, Miller WH, Mader S 2000 Aspartate 351 of estrogen receptor α is not crucial for the antagonist activity of antiestrogens. J Biol Chem 275:20867–20872
20. Levenson AS, Jordan VC 1998 The key to the antiestrogenic mechanism of raloxifene is amino acid 351 (aspartate) in the estrogen receptor. Cancer Res 58:1872–1875
21. Shiau AK, Barstad D, Loria PM, Cheng L, Kushner PJ, Agard DA, Greene GL 1998 The structural basis of estrogen receptor/coactivator recognition and the antagonism of this interaction by tamoxifen. Cell 95:927–937
22. Wolf DM, Jordan VC 1994 The estrogen receptor from a tamoxifen stimulated MCF-7 tumor variant contains a point mutation in the ligand binding domain. Breast Cancer Res Treat 31:129–138
23. Webb P, Nguyen P, Valentine C, Weatherman RV, Scanlan TS, Kushner PJ 2000 An antiestrogen-responsive estrogen receptor-α mutant (D351Y) shows weak AF-2 activity in the presence of tamoxifen. J Biol Chem 275: 37552–37558
24. Yamamoto Y, Wada O, Suzawa M, Yogiashi Y, Yano T, Kato S, Yanagisawa J 2001 The tamoxifen-responsive estrogen receptor α mutant D351Y shows reduced tamoxifen-dependent interaction with corepressor complexes. J Biol Chem 276:42684–42691
25. Chen JD, Evans RM 1995 A transcriptional co-repressor that interacts with nuclear hormone receptors. Nature 377:454–457
26. Voegel JJ, Heine MJ, Zechel C, Chambon P, Gronemeyer H 1996 TIF2, a 160 kDa transcriptional mediator for the ligand-dependent activation function AF-2 of nuclear receptors. EMBO J 15:3667–3675
27. Karvonen U, Janne OA, Palvimo JJ 2002 Pure antiandrogens disrupt the recruitment of coactivator GRIP1 to colocalize with androgen receptor in nuclei. FEBS Lett 523:43–47
28. Black BE, Vitto MJ, Gioeli D, Spencer A, Afshar N, Conaway MR, Weber MJ, Paschal BM 2004 Transient, ligand-dependent arrest of the androgen receptor in subnuclear foci alters phosphorylation and coactivator interactions. Mol Endocrinol 18:834–850
29. Kallenberger BC, Love JD, Chatterjee VK, Schwabe JW 2003 A dynamic mechanism of nuclear receptor activation and its perturbation in a human disease. Nat Struct Biol 10:136–140
30. Kang HY, Yeh S, Fujimoto N, Chang C 1999 Cloning and characterization of human prostate coactivator ARA54, a novel protein that associates with the androgen receptor. J Biol Chem 274:8570–8576
31. Shiau AK, Barstad D, Radek JT, Meyers MJ, Nettles KW, Katzenellenbogen BS, Katzenellenbogen JA, Agard DA, Greene GL 2002 Structural characterization of a subtype-selective ligand reveals a novel mode of estrogen receptor antagonism. Nat Struct Biol 9:359–364
32. Bohl CE, Gao W, Miller DD, Bell CE, Dalton JT 2005 Structural basis for antagonism and resistance of bicalutamide in prostate cancer. Proc Natl Acad Sci USA 102:6201–6206
33. Hara T, Kouno J, Nakamura K, Kusaka M, Yamaoka M 2005 Possible role of adaptive mutation in resistance to antiandrogen in prostate cancer cells. Prostate 65: 268–275
34. Lumbroso S, Lobaccaro JM, Georget V, Leger J, Poujol N, Terouanne B, Evain-Brion D, Czernichow P, Sultan C 1996 A novel substitution (Leu707Arg) in exon 4 of the androgen receptor gene causes complete androgen resistance. J Clin Endocrinol Metab 81:1984–1988
35. Georget V, Terouanne B, Nicolas JC, Sultan C 2002 Mechanism of antiandrogen action: key role of hsp90 in conformational change and transcriptional activity of the androgen receptor. Biochemistry 41:11824–11831
36. van Laar JH, Voorhost-Ogink MM, Zegers ND, Boersma WJA, Claassen E, van der Korput JAGM, Ruizeveld de Winter JA, Van der Kwast TH, Mulder E, Trapman J, Brinkmann AO 1989 Characterization of polyclonal antibodies against the N-terminal domain of the human androgen receptor. Mol Cell Endocr 67:29–38
37. Jones TA, Zou JY, Cowan SW, Kjeldgaard 1991 Improved methods for building protein models in electron density maps and the location of errors in these models. Acta Crystallogr A 47(Pt 2):110–119
38. Brunger AT, Adams PD, Clore GM, DeLano WL, Gros P, Grosse-Kunstleve RW, Jiang JS, Kuszewski J, Nilges M, Pannu NS, Read RJ, Rice LM, Simonson T, Warren GL 1998 Crystallography & NMR system: a new software suite for macromolecular structure determination. Acta Crystallogr D Biol Crystallogr 54(Pt 5):905–921

Molecular Endocrinology **is published monthly by The Endocrine Society (http://www.endo-society.org), the foremost professional society serving the endocrine community.**